Analytical and Numerical Methods in Mechanical Design
Vol.1, Issue 1, Winter & Spring 2022, 57-69

Analysis of Lattice Boltzmann Method for Slip Flow in Trapezoidal Microchannels

Arman Maroufi[1,*], Cyrus Aghanajafi [2] , Jamasb Pirkandi [3]

[1] *Faculty of Industrial and Mechanical Engineering, Islamic Azad University, Qazvin Branch, Qazvin, Iran*
[2]*Department of Mechanical Engineering, K. N. Toosi University of Technology, Tehran, Iran*
[3]*Department of Aerospace Engineering, Malek Ashtar University of Technology, Tehran, Iran*
Received: 19 March 2022- Accepted: 12 May 2022
*Corresponding author: *maroufiqiau@yahoo.com*

Abstract

Two dimensional analysis of fluid flow and heat transfer through the trapezoidal microchannel has been done. The energy and Nervier stokes equations have been solved considering the wall slip velocity and temperature jump using the Lattice Boltzmann method (LBM). The relation between relaxation times and Knudsen number has been derive in LBM. The effects of Reynolds number, Nusslelt number, temperature jump and velocity slip on different Knudsen number ($0.001<Kn<0.1$) and different aspect ratios ($0.2<AR<1.2$) were investigated. The good agreement between results and earlier studies were found. Results show the important effect of AR and Knudsen number on Nusselt number in trapezoidal microchannel. At low Reynolds number the significant influence on Nusselt number has been seen.

***Keywords*:** Trapezoidal microchannel; Lattice Boltzmann method; Knudsen number; Temperature jump

1. Introduction

The vast applications of micro-electro-mechanical systems (MEMS) such as micro heat exchangers, micropumps, biochemical reaction chambers, infrared detectors and medical usage have interested many scientists to simulate their heat transfer and fluid flow behaviors [1-4]. There is diversity between the heat transfer and fluid flow characteristics of microchannels and the normal size channels. When the mean free path of the gas molecules (λ) are not much smaller than the channel dimension, the continuum assumption is not valid. So the effects of surface become important, which change the boundary conditions. In this case, temperature jump and velocity slip take place in the walls. Classification of flow into four regimes was done by Beskok and Karniadakis [5]. They used the Knudsen number for this aim which is defined as:

$$Kn=\lambda/L \quad (1)$$

The flow regimes are free molecular flow ($Kn>10$), transition flow ($0.1<Kn\leq10$), slip flow ($0.001<Kn\leq0.1$), and continuum flow ($Kn\leq0.001$). In this article we study the slip flow regime.

The Navier-Stokes and energy equations are used to model the slip flow and heat transfer. Numerical, experimental and theoretical studies have done by many researchers. Hettiarachchi [6] studied the hydrodynamic and thermal behaviors of rectangular microchannels using FVM. Bin et al. [7] investigated the flow and heat transfer of trapezoidal microchannels with the uniform heat flux boundary condition on the wall. Shams and Shams [8] simulated the slip flow through rhombus microchannels. Wei et al. [9] involved slip flow and temperature jump boundary conditions and modeled the two dimensional, laminar, steady state convective heat transfer for incompressible rarefied gas flow using finite volume, finite difference method. They expressed the Knudsen number effects on Nusselt number under constant wall temperature and heat flux boundary conditions. McHale and Garimellahas [10] studied fully developed laminar flow and Heat transfer in the entrance region of trapezoidal microchannels with no-slip condition. Morini et al. [11] numerically studied the rectangular, trapezoidal and double trapezoidal cross-section mirochannels in the slip flow regime. They presented the role of geometry and Knudsen number on the friction factor. Hong et al. [12] investigated the two-dimensional compressible gaseous flow through parallel plates with constant heat flux. Haddad et al. [13] studied the flow and heat transfer of free gas flow over the

slip flow regime in a parallel-plate microchannel which filled with porous media. They found that the Nusselt number decreases with increasing Knudsen number, thermal conductivity coefficient and Darcy number, while the friction factor increases with Darcy number, Wang et al. [14] studied diatomic gaseous flow and heat transfer in a microchannel with uniform heat flux boundary condition using inverse temperature sampling technique. They showed that the inverse temperature sampling technique accurately simulates the flow and heat transfer of gas. They also showed by increasing the wall heat flux, the rarefaction and compressibility increase with the wall heat flux. Aghanajafi et al. [15] investigated the radiation and convection heat transfer in rhombus microchannels. The lattice Boltzmann method, has gained much attention in fluid dynamics and microchannel simulations, in recent years [16-21]. The LBM has many advantages in Comparison with other numerical methods, such as the easy implementation and calculation procedure, Simplicity in dealing with complex geometries and desirable performance in terms of stability and accuracy [22]. Many researchers are trying to develop lattice Boltzmann method for several boundary condition and new geometries [23-25]. In many of them, the effects of temperature jump and velocity slip have been neglected and none of the articles have studied the trapezoidal microchannels. In this paper the, the laminar incompressible fully developed flow and heat transfer in trapezoidal microchannels taking into account the temperature jump and velocity slip has been studied. The lattice Boltzmann method (LBM) is applied to simulate the flow through trapezoidal microchannel.

2. Governing equation

In this paper, the Boltzmann equation is used to study the thermo-hydrodynamic behavior of flow in microchannel:

$$\frac{\partial n_i}{\partial t}+c_i\frac{\partial n_i}{\partial x_\alpha}=\Omega\left(n_i\right)=-\frac{1}{\tau_n}\left(n_i-n_i^{\,e}\right) \tag{2}$$

$$\frac{\partial f_i}{\partial t}+c_i\frac{\partial f_i}{\partial x_\alpha}=\Omega\left(f_i\right)-n_iZ_i=-\frac{1}{\tau_f}\left(f_i-f_i^{\,e}\right)-n_iZ_i \tag{3}$$

Where n is distribution function for momentum, f is distribution function for energy. n^e nd f^e are equilibrium distribution for momentum and energy respectively. The discrete microscopic velocity is shown as c_i , that can be written as:

$$c_i=\begin{cases}(0,0) & ,\ i=0\\ \left(\cos\frac{i-1}{2}\pi,\sin\frac{i-1}{2}\pi\right)c & ,\ i=1,2,3,4\\ \sqrt{2}\left(\cos\frac{(i-5)}{2}\pi+\frac{\pi}{4},\sin\frac{(i-5)}{2}\pi+\frac{\pi}{4}\right)c, & i=5,6,7,8\end{cases} \tag{4}$$

In eq. (2), Ω is the collision operator, where the BGK [26] model is used in this study. τ_n and τ_f are momentum and internal energy relaxation times respectively.

Here, we used the D_2Q_9 lattice structure which shown in Fig1. The weight functions are selected as:

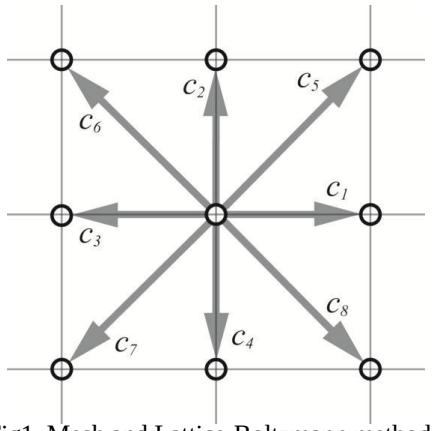

Fig1. Mesh and Lattice-Boltzmann methods

$$w_i = \begin{cases} 4/9 & i = 0 \\ 1/9 & i = 1,2,3,4 \\ 1/36 & i = 5,6,7,8 \end{cases} \tag{5}$$

In eq. (3) the effect of heat dissipation can be written as:

$$Z_i = (c_i - u).D_i u = (c_i - u).\left[\partial_t u + (c_i.\nabla)u\right] \tag{6}$$

We rewrite the Eq. (2) and (3) as below:

$$n_i = n_i + \frac{\Delta t}{2\tau_n}(n_i - n_i^{\,e}) \tag{7}$$

$$\tilde{f_i} = f_i + \frac{\Delta t}{2\tau_f}(f_i - f_i^{\,e}) + \frac{\Delta t}{2} n_i Z_i \tag{8}$$

The equilibrium distribution functions for n and f can be written as follows:

$$n_i^{\,e} = \omega_i \rho[1 + 3\frac{c_i u}{c^2} + 4.5\frac{(c_i u)^2}{c^4} - 1.5\frac{u^2}{c^2}] \tag{9}$$

$$f_i^{\,e} = \begin{cases} -\frac{4}{9}\rho e[1.5\frac{u^2}{c^2}] & , \quad i=0 \\ \frac{1}{9}\rho e[1.5 + 1.5\frac{c_i u}{c^2} + 4.5\frac{(c_i u)^2}{c^4} - 1.5\frac{u^2}{c^2}] & , i=1,2,3,4 \\ \frac{1}{36}\rho e[3 + 6\frac{c_i u}{c^2} + 4.5\frac{(c_i u)^2}{c^4} - 1.5\frac{u^2}{c^2}] & , i=5,6,7,8 \end{cases} \tag{10}$$

The macroscopic characteristics such as density, velocity and internal energy per unit mass can be determined as below:

$$\rho = \sum_i n_i \tag{11}$$

$$\rho u = \sum_i c_i n_i \tag{12}$$

$$\rho e = \sum_i \tilde{f_i} - \frac{\Delta t}{2}\sum_i n_i Z_i \tag{13}$$

The relation between relaxation parameter and Knudsen number can be expressed as:

$$Kn = \sqrt{\frac{\pi\gamma}{2}}\frac{Ma}{\mathrm{Re}} \tag{14}$$

Substituting Mach number and Reynolds number in eq. (14) gives:

$$Kn = \sqrt{\frac{\pi\gamma}{2}} \frac{\left(\frac{u}{c_s}\right)}{\left(\frac{uL}{\upsilon}\right)} \tag{15}$$

Where c_s is the sound speed which given as $c_s = 1/\sqrt{3}$ in LB method and $\upsilon = \tau_f {c_s}^2$. So the relation between Knudsen number and relaxation parameter can be determined as:

$$Kn = \sqrt{\frac{\pi\gamma}{6}} \frac{\tau_f}{L} \tag{16}$$

3. Boundary condition implementation

Constant velocity and temperature profiles are applied at the inlet. Here the non-equilibrium bounce back model is used which proposed by Zou and He [27].

$$\begin{aligned} n_1 &= n_3 + \frac{2}{3}\rho_i u_x \\ n_2 &= n_4 + \frac{2}{3}\rho u_y \\ n_5 &= n_7 + \frac{1}{2}(n_4 - n_2) + \frac{1}{6}\rho_i u_x \\ n_8 &= n_6 - \frac{1}{2}(n_4 - n_2) + \frac{1}{6}\rho_i u_x \end{aligned} \tag{17}$$

In microchannels, the influence of rarefaction should be involved in the slip flow regime. For modeling of velocity slip and temperature jump boundary conditions, here we used the references [28] as below:

$$u_0^{slip} = u_0 - u_{wall} = \frac{2-\sigma_v}{\sigma_v} Kn \left(\frac{\partial u}{\partial y}\right)_{y=0} \tag{18}$$

$$u_H^{slip} = u_{wall} - u_H = \frac{2-\sigma_v}{\sigma_v} Kn \left(\frac{\partial u}{\partial y}\right)_{y=H} \tag{19}$$

$$T_0^{slip} = T_0 - T_{wall} = \frac{2-\alpha_T}{\alpha_T}\left(\frac{2k}{k+1}\right)\left(\frac{Kn}{\mathrm{Pr}}\right)\left(\frac{\partial T}{\partial y}\right)_{y=0} \tag{20}$$

$$T_H^{slip} = T_{wall} - T_H = \frac{2-\alpha_T}{\alpha_T}\left(\frac{2k}{k+1}\right)\left(\frac{Kn}{\mathrm{Pr}}\right)\left(\frac{\partial T}{\partial y}\right)_{y=H} \tag{21}$$

Where σ_v and α_T are defined as the tangential momentum and thermal accommodation coefficient respectively. These coefficients are assigned to one that means all the molecules which hitting the wall are completely diffusively reflected back. For implying boundary conditions for trapezoidal geometry we use Guo et al research [29]. As shown in Fig. (2), the link between the fluid and wall nodes $(x_f \ and \ x_w)$ intersects the physical boundary at x_w. The velocity is given as:

$$u = \begin{cases} u_{w1} & , \Delta \geq 0.75 \\ \Delta u_{w1} + (1-\Delta) u_{w2} & , \Delta < 0.75 \end{cases} \tag{22}$$

Where

$$\Delta = \frac{|x_f - x_b|}{|x_f - x_w|} \tag{23}$$

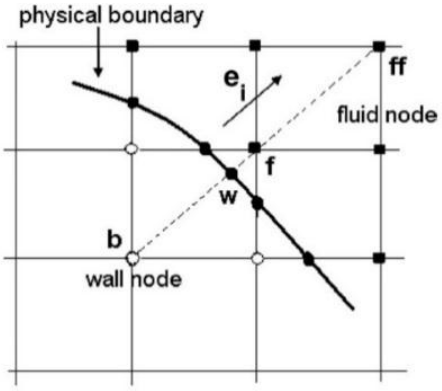

Fig. 2. The geometry condition of curved wall boundary.

4. Numerical model

The schematic of trapezoidal microchannel is shown in Fig (3). The definition of the aspect ratio of microchannel is as below:

$$AR = \frac{H}{b} \tag{24}$$

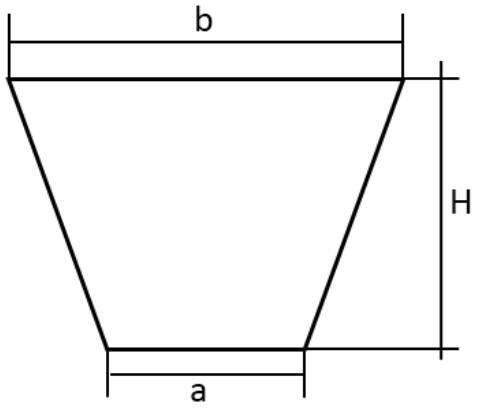

Fig. 3. A schematic of the trapezoidal channel.

It is varied from 0.25 to 1.2. The length of the microchannel considered sufficiently long, to reach the fully developed condition. The governing characteristics for solving method are continuity, momentum and energy equations with the LBM.

5. Validation of numerical approach

To reach the convergence of the solution the residuals are considered 10-6 which gives accurate results. To ensure that the solution is independent of the lattice size the grid independency check has been done. The 31*31, 51*51, 71*71 and 101*101 lattice have been choosing. It was observed that the optimum size of lattices is 71*71 and making the lattices thinner would not increase the preciseness. Here, some comparisons have been done to show the numerical method, models the slip flow regime accurately. First the results for Poiseuille number compared with the analytical solution for different Knudsen numbers in Table 1 and the results were in good agreement with the analytical solution. Second, the results for Nusselt numbers compared with the results of reference [30] for different Reynolds number in Table 2. At last, for different aspect ratios and Knudsen number the amount of Poiseuille number compared with the results of reference [11] in Table 3.

All the results were agreeing with the results of reference [30] and [11] acceptably. To establish that the numerical procedure accurately models the slip flow regime, some comparisons are performed. Poiseuille numbers have been compared with analytical values according to Po=24/(1+12Kn) in Table 1, and the results shows acceptable agreement. In Table 2, the Nusselt numbers have been compared with the results of Reinksizbulut's study [20] for Kn=0, through a range of Reynolds numbers. The comparisons have been performed for parallel plates. The aspect ratio has been chosen sufficiently large that the channel geometry tends to parallel plates.

Another case of validation is presented in Table 3 in which contains the outcomes of this research and the outcomes of Morini [11]. The results are completely agreeing with the Morini's results for different value of Φ (Φ is the ratio of Poiseuille number at Kn=0 to Poiseuille number at non-zero Kn).

Table 1. The Poiseuille number for fully developed flow in parallel plates.

Knudsen Number	Poiseuille number (results of analytical solution)	Present results	Error %
0	24	23.9761	0.1
0.005	22.64	22.612	0.12
0.01	21.43	21.3524	0.36
0.05	15	15.065	0.4
0.1	10.91	10.986	0.64

Table 2. The Nusselt number for parallel plates in fully developed flow.

Reynolds number	Results of ref[30]	Present results	**Error %**
0.1	8.105	8.12	0.18
1	8	8.039	0.5
5	7.741	7.8	0.77
10	7.624	7.65	0.3

Table 3. The Poiseuille number for trapezoidal microchannel in fully developed flow.

Aspect ratio	*Kn=0*		*Kn=0.001*	
AR	Result of [11] (φ)	Present result (φ)	Result of [11] (φ)	Present result (φ)
0.7	14.690	14.654	0.991	0.992
1	14.063	14.030	0.992	0.992
1.25	13.832	13.802	0.992	0.998
Aspect ratio	Kn=0.01		Kn=0.1	
AR	Result of [11] (φ)	Present result (φ)	Result of [11] (φ)	Present result (φ)
0.7	0.922	0.929	0.545	0.553
1	0.924	0.926	0.555	0.563
1.25	0.925	0.923	0.559	0.564

6. Results and discussion

In this section, the effects of rarefaction, geometry and Reynolds, Poiseuille and Nusselt numbers are presented within three subsections.

6.1. Validation of slip flow condition

In the Fig. (4), the variation of Knudsen number with length of microchannel for different Aspect ratios at R=40 has been shown. It is seen that the Knudsen numbers are in the range of slip flow (0.001<Kn<0.1), therefore, this modeling can be continued by this assumption that the slip flow condition is accurate for these aspect ratios of this study. The other result from this figure is that in all of aspect ratios, the Knudsen number is less than 0.01 in the first half of the microchannel. But after the middle of the microchannle, the Knudsen number increase suddenly.

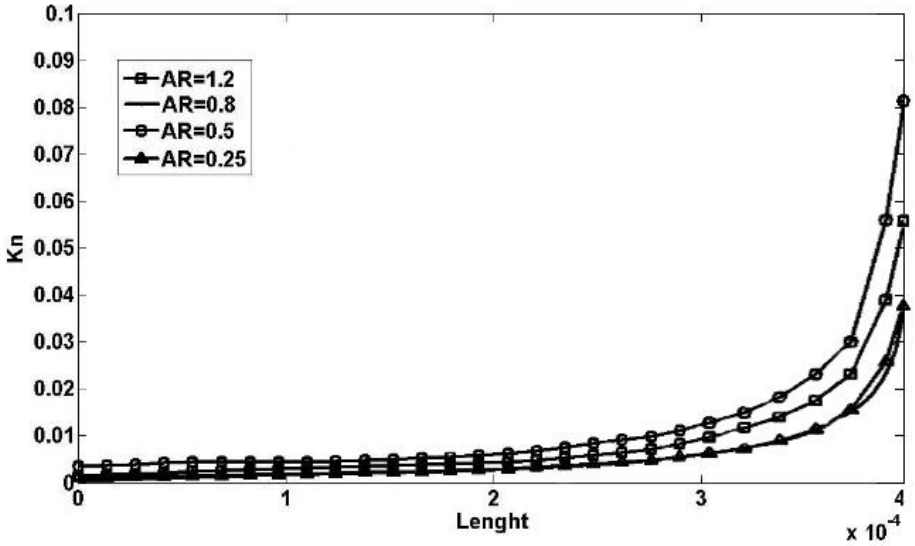

Fig. 4. Variation of Knudsen number with Length of microchannel on the wall for different aspect ratios at Re=40.

Fig. (5) shows the range of the Knudsen number quantity with the Reynolds numbers variation for the aspect ratio of 0.5. These changes show that by decreasing the Reynolds number, the assumption of slip flow in this study for all cases may be inaccurate. Therefore, it can be written that in the Reynolds numbers of 10, 30, and 40, the slip flow assumption is acceptable and in the Reynolds numbers below 1, the slip flow assumption is inaccurate.

The velocity profiles for the Reynolds numbers of 10, 30, and 40, show that in the fully developed section of microchannel, the flow regime is in the slip condition for all the aspect ratios.

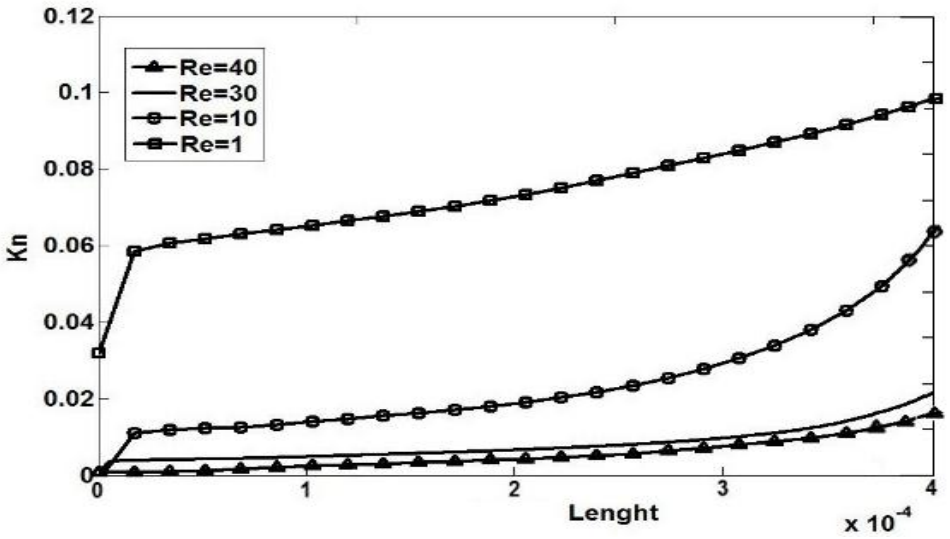

Fig. 5. Variation of Knudsen number with Length of microchannel on the wall for different Reynolds numbers at

6.2 Poiseuille number

In the Fig. (6), the variation of fully developed poiseuille numbers with aspect ratios for different Reynolds numbers is shown. The Poiseuille number is increased by increasing the aspect ratio in all of the Reynolds numbers. This means that by increasing the area of cross section, the Poiseuille number of fully developed section is decreased while the hydraulic diameter is approximately at a fixed amount. An important result of this figure is that by changing the Reynolds numbers, the graph of Poiseuille number has insensitive change, and this means that changing the Reynolds number has meaningless effect on Poiseuille number.

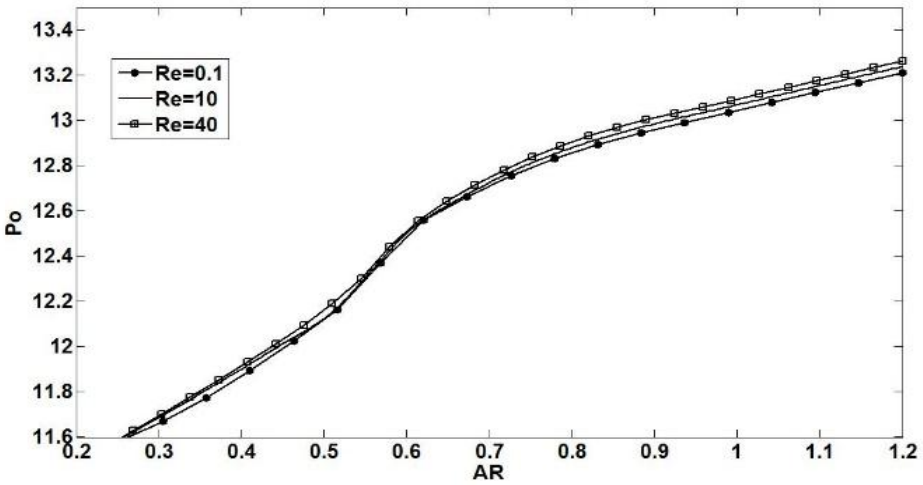

Fig 6. Variation of fully developed poiseuille number with aspect ratio for different Reynolds numbers.

6.3. Nusselt number

The most important parameter in heat transfer is the ratio of convective to conductive heat transfer across the boundary, which is called the Nusselt number. Fig. (7) represents the variation of Nusselt number with the aspect ratio for different Reynolds number at Pr=0.74. It can be concluded that by I creasing the aspect ratio, the Nusselt number increases.

This means that by increasing the area of cross section, the Nusselt number of fully developed section is decreased while the hydraulic diameter is approximately at a fixed amount. Also it is clear that the acceleration of increasing of Nusselt number is different before and after of the aspect ratio of 0.5. Before aspect ratio of 0.5, the Nusselt number is increased by a less growth rate. The other important result from this figure is that the rate of increasing the Nusselt number is a function of Reynolds number (by direct relation to this number). For considering the effects of different situation of temperature on the Nusselt number, a new indicator (temperature indicator) has been identified as below:

$$\theta = \left(T_{inlet} - T_{wall}\right) / T_{wall}$$

(25)

In the Fig. (8) the Variation of Nusselt number with aspect ratio for different temperature at Pr=0.74 and Re=40 is shown. It can be seen that by increasing the aspect ratio and decreasing the area of cross section, the Nusselt number is increases in the fully developed section of the microchannel. The most important result of this figure is that by increasing the temperature indicator (θ), the Nusselt number is increased also it is clear that the rate of increasing of Nesselt number is higher than the rate of increasing in the temperature indicator (θ).

Fig. (9) shows the variation of Nusselt number with Knudsen number at Re=1 at Pr=0.74 for different temperature indicators (θ). This figure shows that in the low aspect ratios, the Nusselt number is low and meaningless, and for aspect ratios more than 0.8 the Nusselt number suddenly increases. The other noticeable result from this figure is that the Nusselt number has and direct relationship to the temperature indicator (θ). By increasing the temperature indicator (θ), the Nusselt number increases at a higher rate.

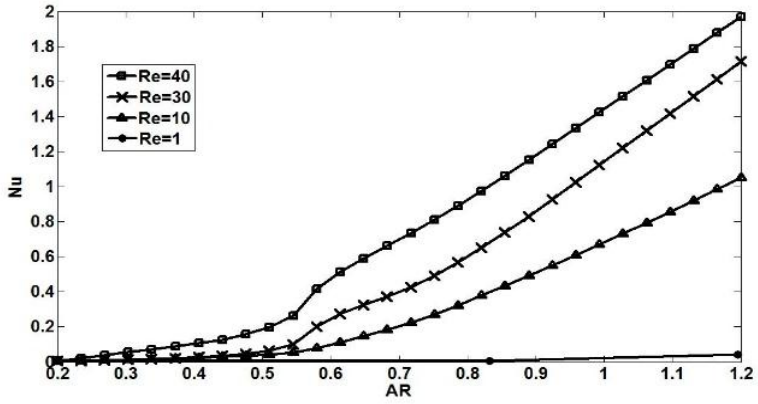

Fig. 7. Variation of Nusselt number with aspect ratio for different Reynolds numbers at Pr=0.74

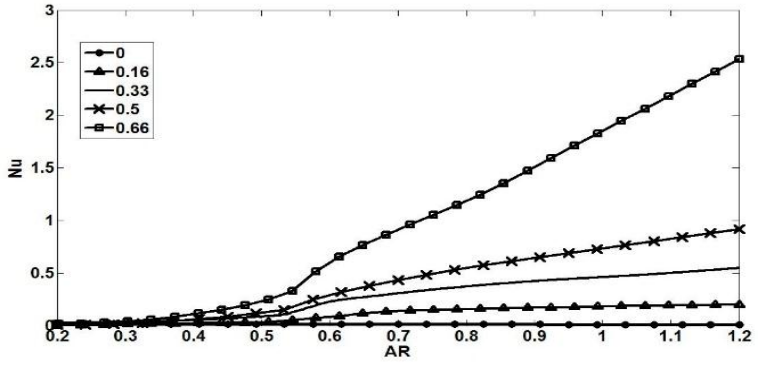

Fig. 8. Variation of Nusselt number with aspect ratio for different (θ) at Pr=0.74, and Re=40.

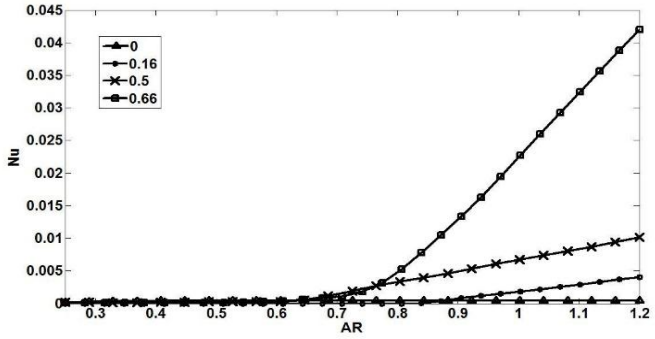

Fig. 9. Variation of Nusselt number with Knudsen number for different (θ) at Re=1 Pr=0.74

Table 4. Variation of Nusselt number, Knudsen number, Prandtl number, and Poiseuille number in the case of Re=40 and θ=0.66 of trapezoidal microchannel.

AR	*Nu*	*Kn*	*Pr*	*Po*
1.209	1.992	0.004	10.820	13.271
0.801	0.928	0.002	21.284	12.922
0.602	0.493	0.009	4.612	12.483
0.505	0.188	0.10	4.011	12.172
0.252	0.037	0.005	8.598	11.582

Table 5. Variation of Nusselt number, Knudsen number, Prandtl number, and Poiseuille number in the case of Re=1 and θ=0.66 of trapezoidal microchannel.

AR	*Nu*	*Kn*	*Pr*	*Po*
1.21	0.04	0.12	0.42	13.23
0.80	0.00	0.59	0.69	12.87
0.60	0.00	0.07	0.61	12.51
0.51	0.00	0.17	0.24	12.13
0.25	0.00	0.24	0.17	11.58

By comparing the Figures 8 and 9, it is clear that by increasing the aspect ratio and increasing the Reynolds number, the Nusselt number has a noticeable amount. It has to been highlighted that in all of cases of aspect ratios, the temperature indicator (θ) has an important effect on the Nusselt number. By increasing this factor, the Nusselt number is increased more and more.

In the Fig. (10) the variation of Nusselt number with Knudsen number for different temperature indicators (θ) at Re=40 and Pr=0.74 is shown. It can be seen that the Nusselt number increases by decreasing the Knudsen number. The other outcome of this figure is that the Nusselt number increases by increasing the temperature indicator (θ). An important result of this figure is that by increasing the Knudsen number, the Nusselt number drops suddenly and after that for most of Knudsen numbers, the Nusselt number drop smoothly.

Table 4 shows (in the case of Re=40 and, θ=0.66) that by increasing the aspect ratio in the trapezoidal microchannel, the Nusselt number is increased, the Knudsen number is at the slip flow regime, the Prandtl Number increases and after that has a drop, and finally the Poiseuille number is increased.

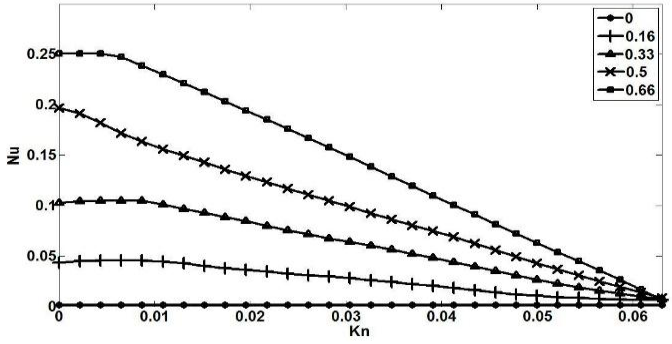

Fig. 10. Variation of Nusselt number with Knudsen number for different temperatures at Re=40 and Pr=0.74.

In the case of Re=1 and θ=0.66 table 5 indicates that by increasing the aspect ratio in the trapezoidal microchannels, the Nusselt number is approximately zero and the Knudsen number, is approximately out of the slip flow condition in all of cases. Also the Prandtl number go upward and increases until the aspect ratio of 0.8. After that, it has a drop, and finally Poiseuille number has the amounts near to the case of Re=40 and θ=0.66.

7. Conclusions

In this study the fully developed laminar flow in trapezoidal mirochannels is investigated using the LBM and the temperature-jump and constant wall temperature boundary conditions were included. The effects of Reynolds number, Nusslelt number on different Knudsen number (0.001<Kn<0.1) and different aspect ratios (0.2<AR<1.2) were investigated. The results show that the Reynolds number has more effect on the Nusselt number in comparison with the Poiseuille number especially in low Reynolds number. by decreasing the amount of aspect ratio, The Poiseuille and Nusselt numbers both decrease, but rarefaction has inverse effect on Nusselt and Poiseuille number in which Nusselt and Poiseuille numbers decreases with increasing in Knudsen number fast in the first section then smoothly. It can be seen from the figures that the Reynolds number has more effect on Nusselt number than Poiseuille number. Increasing of Nusselt number by increasing aspect ratio has a different manner. It increases smoothly then increasing fast. In addition, Nusselt number is increased by increasing the temperature indicator (θ). Decreasing the Reynolds number increases Knudsen number therefore the change of flow from the slip flow condition will happen.

References

[1] Mavriplis, C., J. C. Ahn, and R. Goulard. "Heat transfer and flow fields in short micro channels using direct simulation Monte Carlo." Journal of Thermophysics and Heat Transfer 11.4 (1997): 489-496.

[2] Jiang, Pei-Xue, et al. "Thermal–hydraulic performance of small scale micro-channel and porous media heat-exchangers." International Journal of Heat and Mass Transfer 44.5 (2001): 1039-1051.

[3] Muzychka, Y. S. "Constructed multi-scale design of compact micro-tube heat sinks and heat exchangers." International journal of thermal sciences 46.3 (2007): 245-252.

[4] Srinivasan, Ravi, et al. "Micro machined reactors for catalytic partial oxidation reactions." AIChE Journal 43.11 (1997): 3059-3069.

[5] Beskok, Ali, and George E. Karniadakis. Simulation of heat and momentum transfer in complex microgeometries. MS thesis. Princeton University, 1994.

[6] Hettiarachchi, HD Madhawa, et al. "Three-dimensional laminar slip-flow and heat transfer in a rectangular microchannel with constant wall temperature." International Journal of Heat and Mass Transfer 51.21 (2008): 5088-5096.

[7] Cao, Bin, Guang Wen Chen, and Quan Yuan. "Fully developed laminar flow and heat transfer in smooth trapezoidal microchannel." International communications in heat and mass transfer 32.9 (2005): 1211-1220.

[8] Shams, M., et al. "Numerical simulation of slip flow through rhombus microchannels." International Communications in Heat and Mass Transfer36.10 (2009): 1075-1081.

[9] Sun, Wei, Sadik Kakac, and Almila G. Yazicioglu. "A numerical study of single-phase convective heat transfer in microtubes for slip flow." International Journal of Thermal Sciences 46.11 (2007): 1084-1094.

[10]McHale, John P., and Suresh V. Garimella. "Heat transfer in trapezoidal microchannels of various aspect ratios." International Journal of Heat and Mass Transfer 53.1 (2010): 365-375.

[11]Morini, Gian Luca, M. Spiga, and P. Tartarini. "The rarefaction effect on the friction factor of gas flow in

microchannels." Superlattices and microstructures 35.3 (2004): 587-599.

[12]Hong, Chungpyo, Yutaka Asako, and Jae-Heon Lee. "Heat transfer characteristics of gaseous flows in micro-channel with constant heat flux." International Journal of Thermal Sciences 46.11 (2007):1153-1162.

[13]Haddad, O. M., M. M. Abuzaid, and M. A. Al-Nimr. "Developing free-convection gas flow in a vertical open-ended microchannel filled with porous media." Numerical Heat Transfer, Part A: Applications 48.7 (2005): 693-710.

[14]Wang, Qiu-Wang, et al. "Numerical investigation of rarefied diatomic gas flow and heat transfer in a microchannel using DSMC with uniform heat flux boundary condition—Part I: numerical method and validation." Numerical Heat Transfer, Part B: Fundamentals 53.2 (2007): 160-173.

[15]Aghanajafi, C., V. Vandadi, and M. R. Shahnazari. "Investigation of convection and radiation heat transfer in rhombus microchannels." IJRRAS3.2 (2010): 167-176.

[16]Bo, Zheng, et al. "Numerical study on the pressure drop of fluid flow in rough microchannels via the lattice Boltzmann method." International Journal of Numerical Methods for Heat & Fluid Flow 25.8 (2015): 2022-2031.

[17]Nayak, Rajlakshmi, et al. "Flow and Thermal Transport Studies in Microchannel Flows using Lattice Boltzmann Method." International Journal of Micro-Nano Scale Transport (2014).

[18]Esfahanian, V., E. Dehdashti, and A. M. Dehrouyeh-Semnani. "Fluid-Structure Interaction in microchannel using Lattice Boltzmann method and size-dependent beam element." Advances in Applied Mathematics and Mechanics 6.3 (2014): 345-358.

[19]Bakhshan, Younes, and Alireza Omidvar. "Calculation of friction coefficient and analysis of fluid flow in a stepped micro-channel for wide range of Knudsen number using Lattice Boltzmann (MRT) method." Physica A: Statistical Mechanics and its Applications 440 (2015): 161-175.

[20]Zarita, Rahouadja, and Madjid Hachemi. "Microchannel fluid flow and heat transfer by lattice boltzmann method." (2014).

[21]Karimipour, Arash. "New correlation for Nusselt number of nanofluid with Ag/Al 2 O 3/Cu nanoparticles in a microchannel considering slip velocity and temperature jump by using lattice Boltzmann method." International Journal of Thermal Sciences 91 (2015): 146-156.

[22]Maroufi, Arman, and Cyrus Aghanajafi. "Analysis of conduction–radiation heat transfer during phase change process of semitransparent materials using lattice Boltzmann method." Journal of Quantitative Spectroscopy and Radiative Transfer 116 (2013): 145-155.

[23]Liou, Tong-Miin, and Chin-Tien Lin. "Three-dimensional rarefied gas flows in constricted microchannels with different aspect ratios: asymmetry bifurcations and secondary flows." Microfluidics and Nanofluidics 18.2 (2015): 279-292.

[24]Taher, M. A., L. K. Saha, and Y. W. Lee. "Effects of Circular Riblets Rough Microchannel on Friction and Fluid Flow using LBM." Procedia Engineering105 (2015): 425-430.

[25]Kuzmin, A., M. Januszewski, D. Eskin, F. Mostowfi, and J. J. Derksen. "Three-dimensional binaryliquid lattice Boltzmann simulation of microchannels with rectangular cross sections." Chemical engineering journal178 (2011): 306-316.

[26]Qian, Y. H., Dominique d'Humières, and Pierre Lallemand. "Lattice BGK models for Navier-Stokes equation." EPL (Europhysics Letters) 17.6 (1992): 479.

[27]Zou, Qisu, and Xiaoyi He. "On pressure and velocity boundary conditions for the lattice Boltzmann BGK model." Physics of fluids 9.6 (1997): 1591-1598.

[28]Chen, Sheng, and Zhiwei Tian. "Simulation of microchannel flow using the lattice Boltzmann method." Physica A:

Statistical Mechanics and its Applications 388.23 (2009): 4803-4810.

[29]Guo, Zhaoli, Chuguang Zheng, and Baochang Shi. "An extrapolation method for boundary conditions in lattice Boltzmann method." Physics of Fluids 14.6 (2002): 2007-2010.

[30]Renksizbulut, Metin, H. Niazmand, and G. Tercan. "Slip-flow and heat transfer in rectangular microchannels with constant wall temperature." International Journal of Thermal Sciences 45.9 (2006): 870-881.